Bartlett *et al*. 10.1073/pnas.0707461104.

Supporting Information

Files in this Data Supplement:

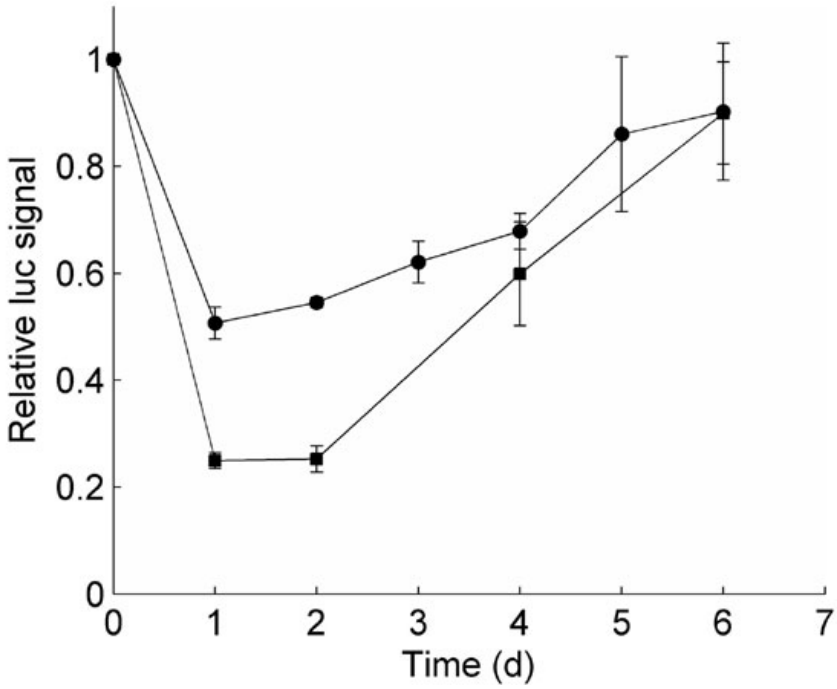

Fig. 5.
Luciferase knockdown by unmodified and DOTA-conjugated siRNA in luciferase-expressing Neuro2A-Luc cells. Luciferase knockdown is reported relative to the luciferase activity from cells transfected with equal doses of the siCON control sequence. Circles, DOTA-siRNA; squares, unmodified siRNA. Error bars = SD.

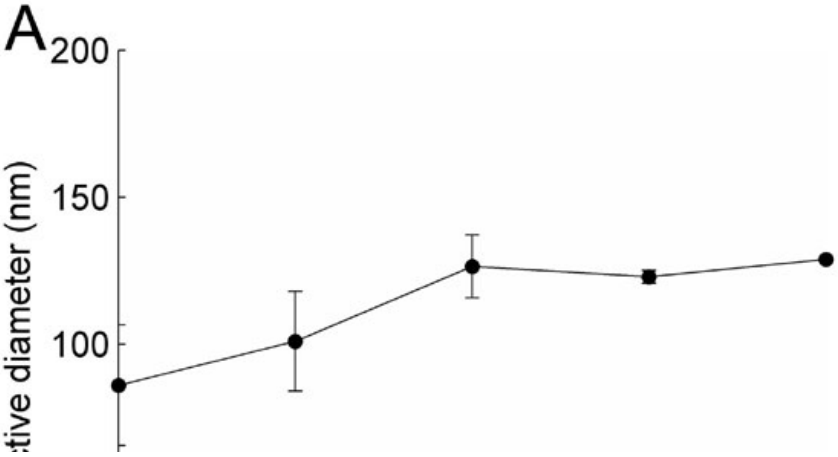

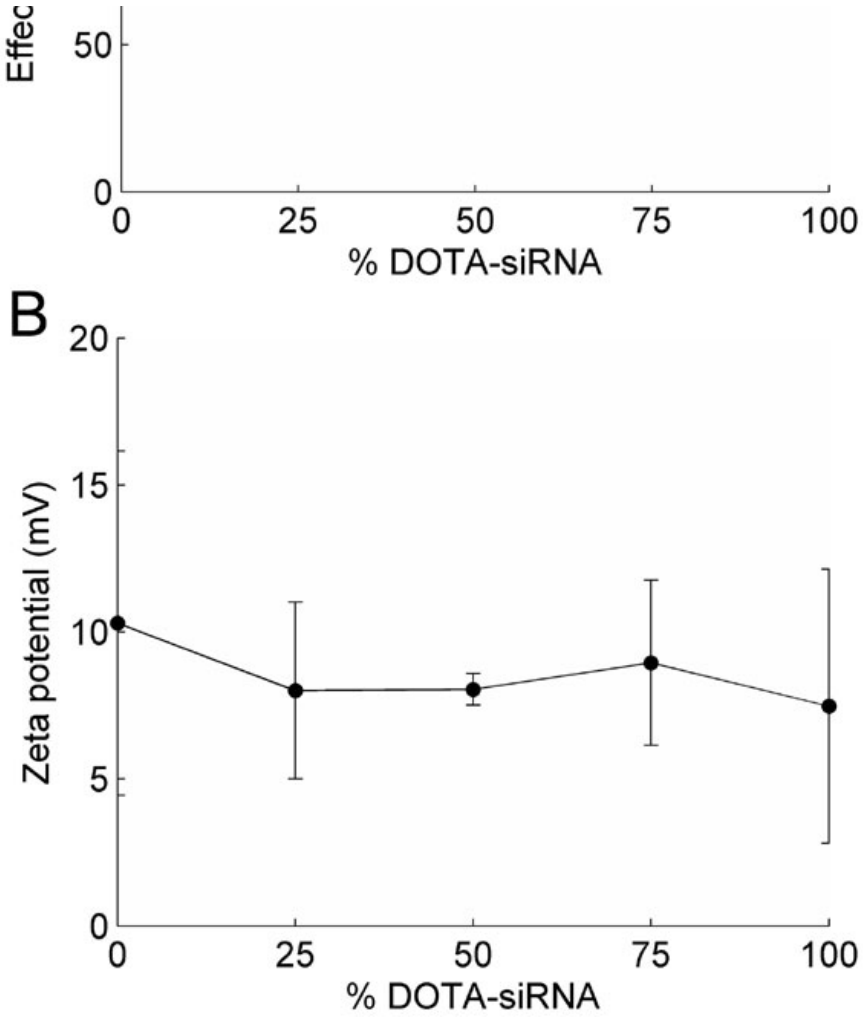

Fig. 6. Properties of nanoparticles formed with 0 to 100% DOTA-siRNA. (*A*) Effective hydrodynamic diameter. (*B*) Zeta potential. Error bars = SD.

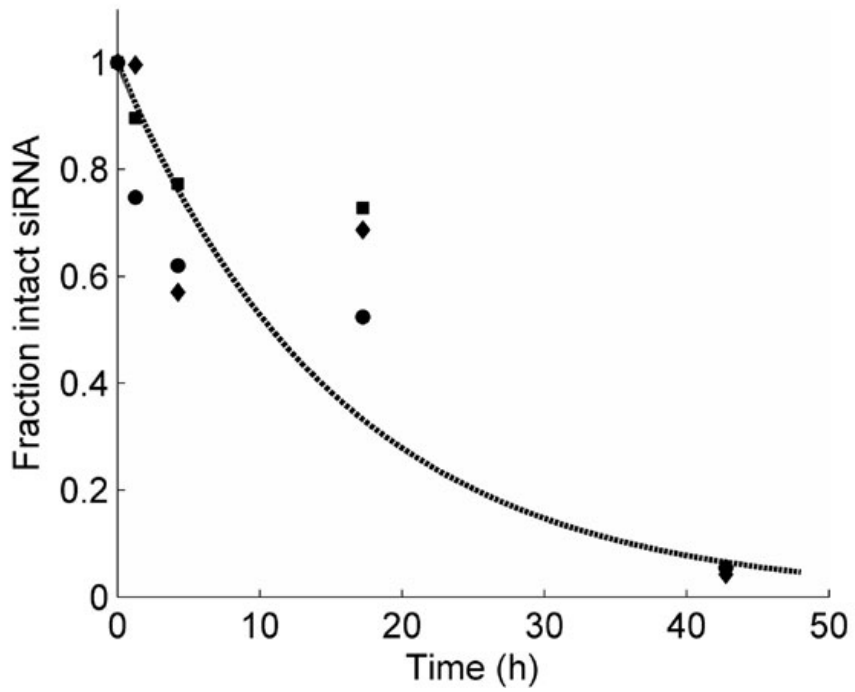

Fig. 7. Nuclease stability of nanoparticle-encapsulated siRNA after incubation at 37 °C and 5% CO_2 in 50% mouse serum. After gel electrophoresis, band intensities were quantified with ImageJ software and plotted versus time to estimate the degradation half-life of the encapsulated siRNA. Circles, nanoparticles formed with unmodified siRNA; diamonds, nanoparticles formed with 20% DOTA-siRNA; squares, nanoparticles formed with 50% DOTA-siRNA.

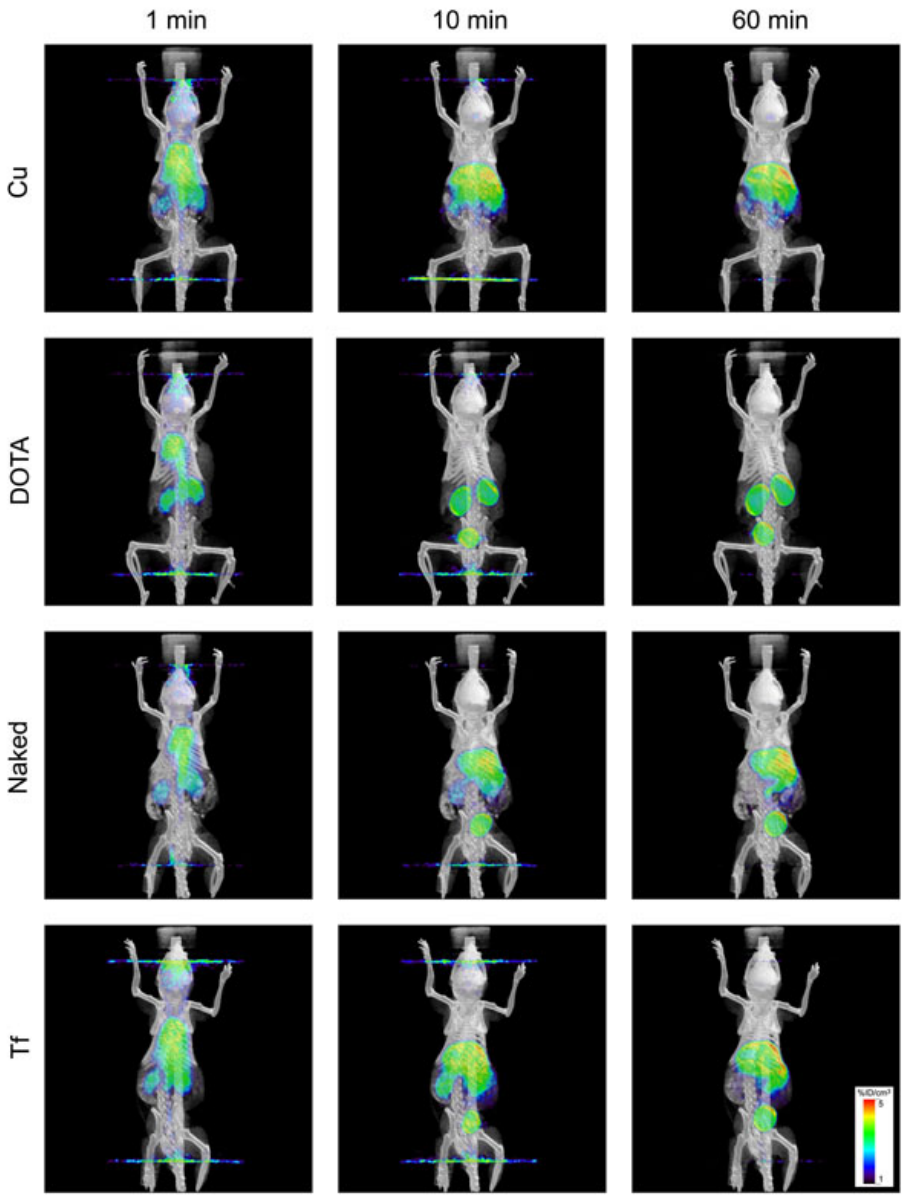

Fig. 8. Fused microPET/CT images of mice at 1, 10, and 60 min after i.v. injection. Images are shown for mice injected with free ^{64}Cu (Cu), ^{64}Cu-labeled DOTA (DOTA), ^{64}Cu-labeled DOTA-siRNA (Naked), and Tf-targeted nanoparticles (Tf) containing ≈50% ^{64}Cu-labeled DOTA-siRNA. All images are displayed on the same scale (min threshold = 1%ID/cm^3; max threshold = 5%ID/cm^3).

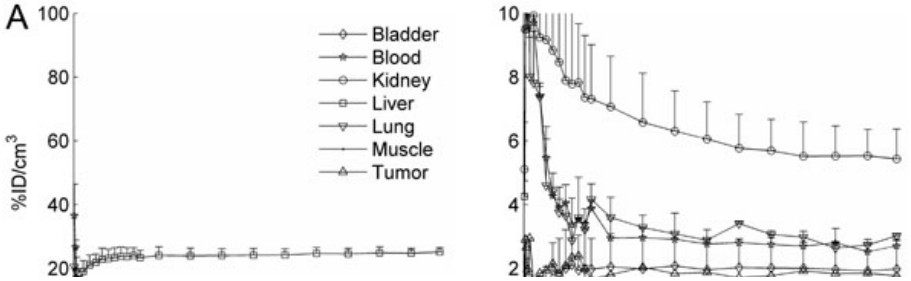

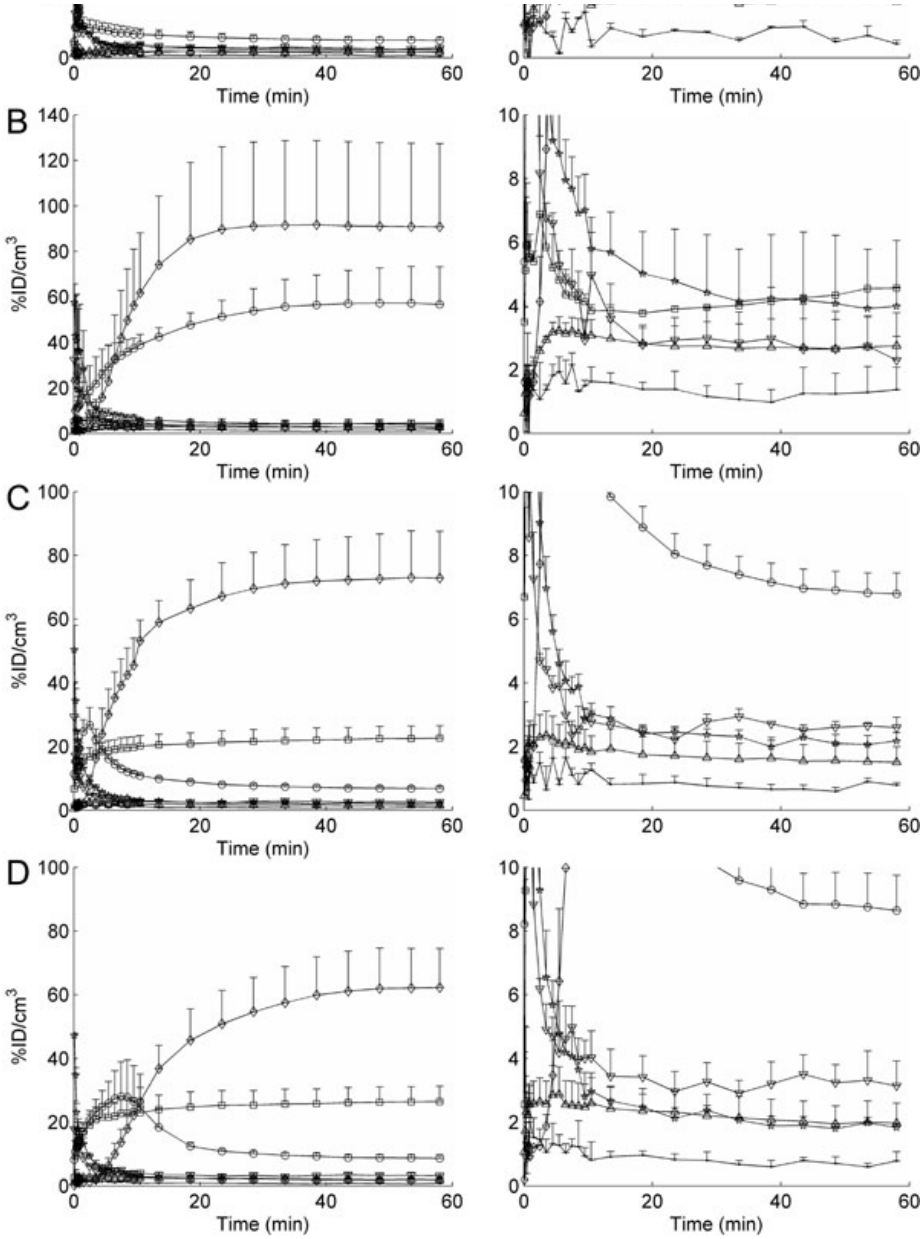

Fig. 9. Average time-activity curves for the first 60 min after i.v. injection. Data are shown for mice injected with ^{64}Cu (*A*), ^{64}Cu-labeled DOTA (*B*), ^{64}Cu-labeled DOTA-siRNA (*C*), and Tf-targeted nanoparticles (*D*) containing ≈50% ^{64}Cu-labeled DOTA-siRNA. Regions of interest (ROI) were drawn within each tissue or organ and the %ID/cm^3 for each ROI was calculated over all time frames using AMIDE software. Error bars = SE.

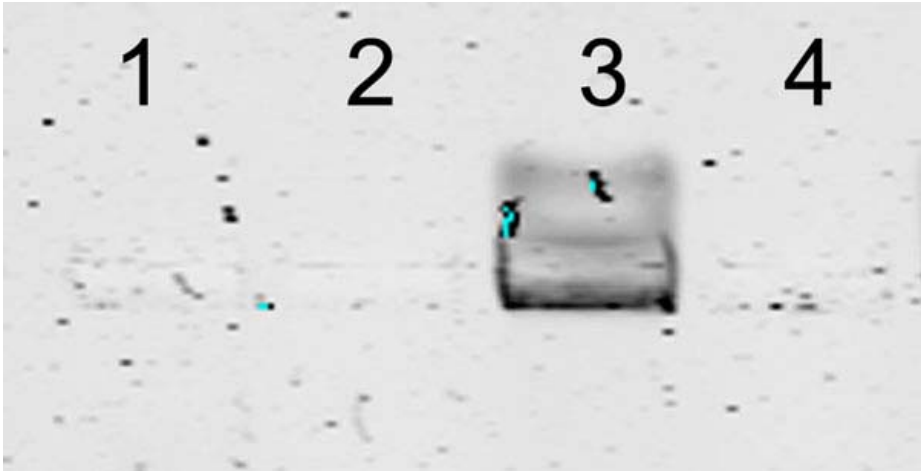

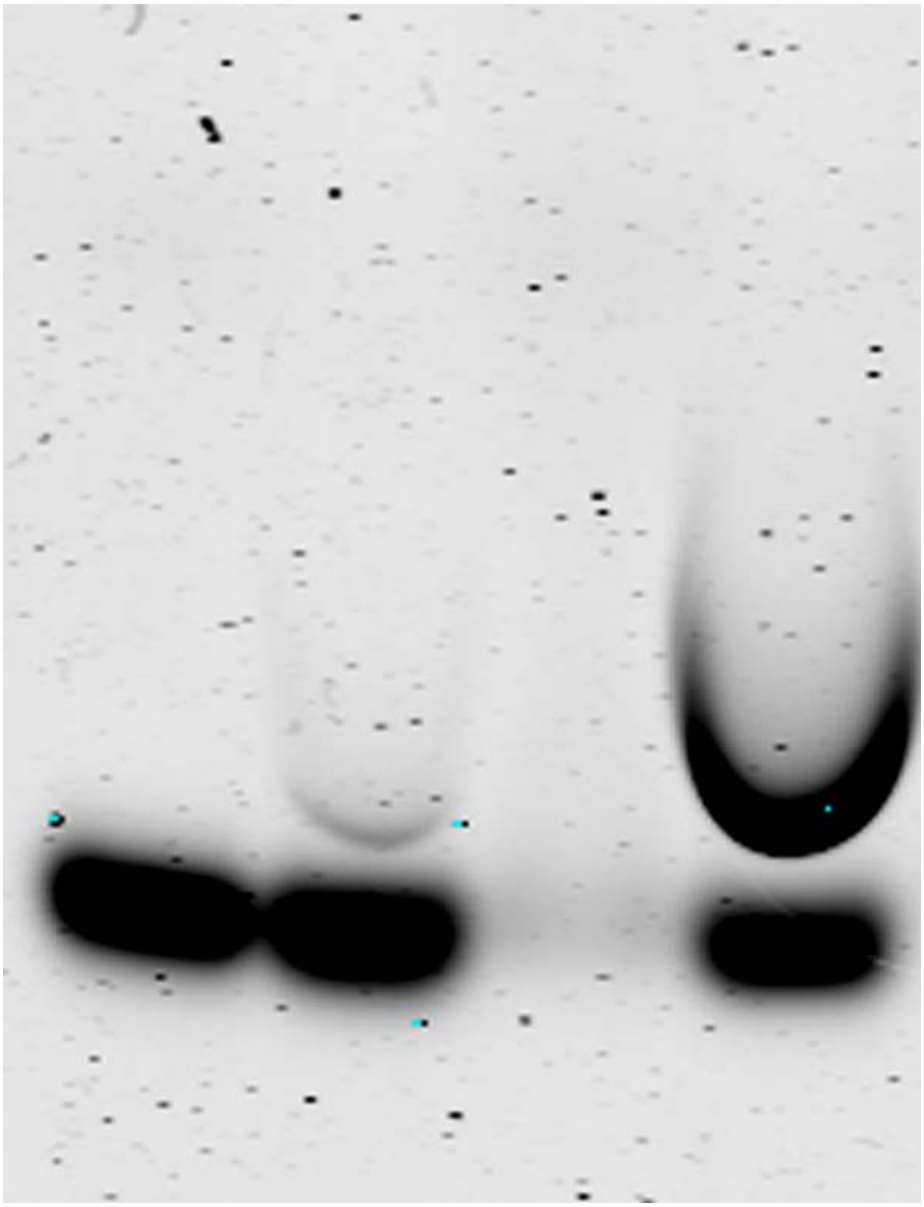

Fig. 10. Gel electrophoresis analysis of ^{64}Cu-DOTA-siRNA nanoparticles before injection for microPET/CT imaging. Lane 1 = ^{64}Cu-DOTA-siRNA; lane 2, ^{64}Cu-DOTA-siRNA + 1% SDS; lane 3, ^{64}Cu-DOTA-siRNA packaged into Tf-targeted nanoparticles (charge ratio (+/-) = 3); lane 4, ^{64}Cu-DOTA-siRNA packaged into Tf-targeted nanoparticles (charge ratio (+/-) = 3) + 1% SDS.

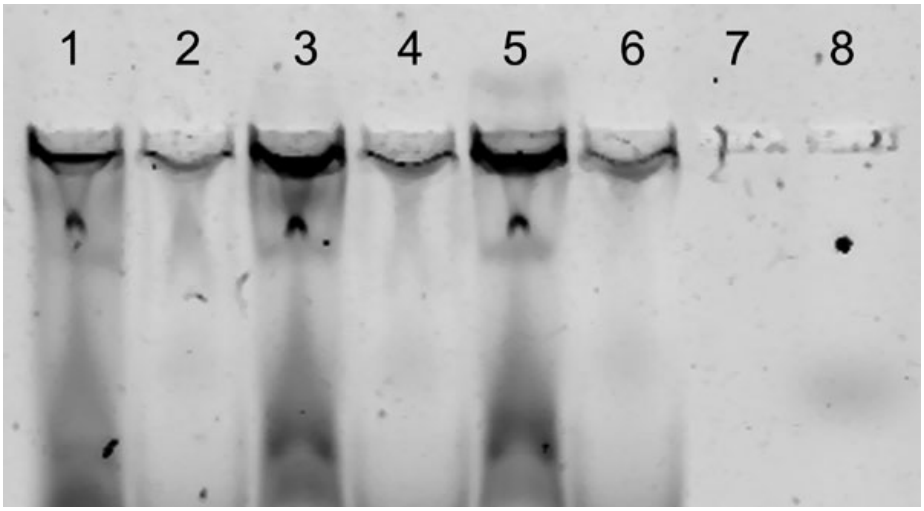

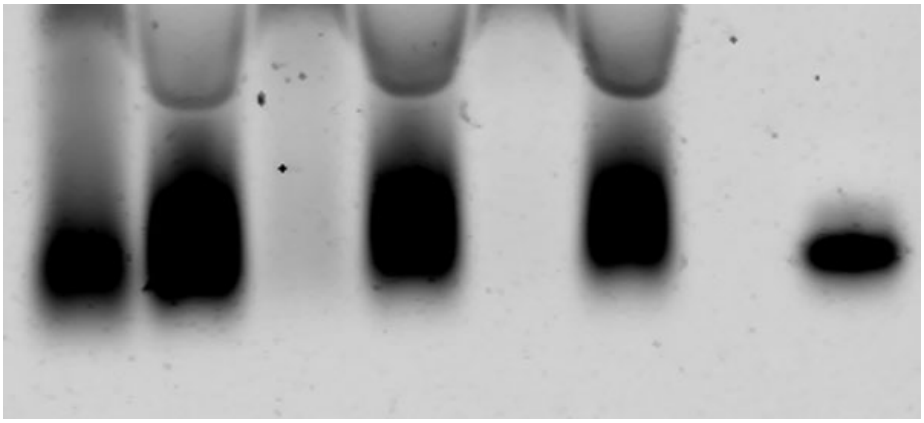

Fig. 11. Gel electrophoresis analysis of ^{64}Cu-DOTA-siRNA nanoparticles incubated for ≈5 min in fresh whole mouse blood. Lane 1, ^{64}Cu-DOTA-siRNA + whole mouse blood; lane 2, ^{64}Cu-DOTA-siRNA + 1% SDS + whole mouse blood; lane 3, ^{64}Cu-DOTA-siRNA packaged into Tf-targeted nanoparticles (charge ratio (+/-) = 3) + whole mouse blood; lane 4, ^{64}Cu-DOTA-siRNA packaged into Tf-targeted nanoparticles (charge ratio (+/-) = 3) + 1% SDS + whole mouse blood; lane 5, ^{64}Cu-DOTA-siRNA packaged into Tf-targeted nanoparticles (charge ratio (+/-) = 6) + whole mouse blood; lane 6, ^{64}Cu-DOTA-siRNA packaged into Tf-targeted nanoparticles (charge ratio (+/-) = 6) + 1% SDS + whole mouse blood; lane 7, empty; lane 8, ^{64}Cu-DOTA-siRNA in water.

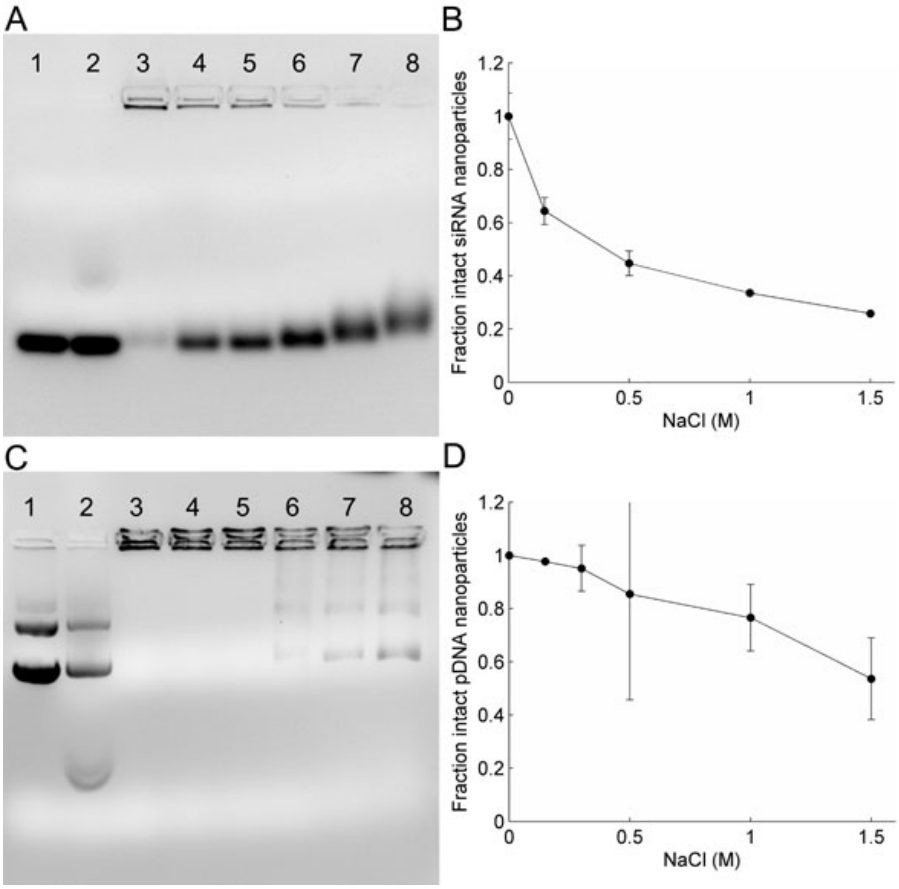

Fig. 12. NaCl concentration-dependent disruption of Tf-targeted nanoparticles containing unmodified siRNA. (*A*) Gel electrophoresis of siRNA nanoparticles: lane 1, naked siRNA; lane 2 = nanoparticles + 1% SDS; lane 3, nanoparticles in water; lane 4, nanoparticles in 1X PBS; lane 5, nanoparticles in 0.15 M NaCl; lane 6, nanoparticles in 0.5 M NaCl; lane 7, nanoparticles in 1 M NaCl; lane 8, nanoparticles in 1.5 M NaCl. (*B*) Fraction of intact siRNA nanoparticles based on intensity in the wells (corresponding to siRNA within intact nanoparticles). The change in intensity with increasing NaCl concentration was normalized to the intensity for siRNA nanoparticles incubated in water alone (lane 3). Error bars = SD. (*C*) Gel electrophoresis of pDNA nanoparticles: lane 1 = naked pDNA; lane 2, nanoparticles + 1% SDS; lane 3, nanoparticles in water; lane 4, nan oparticles in 0.15 M NaCl; lane 5, nanoparticles in 0.3 M NaCl; lane 6, nanoparticles in 0.5 M NaCl; lane 7, nanoparticles in 1 M NaCl; lane 8, nanoparticles in 1.5 M NaCl. (*D*) Fraction of intact pDNA nanoparticles based on intensity in the wells (corresponding to pDNA within intact nanoparticles). The change in intensity with increasing NaCl concentration was normalized to the intensity for pDNA nanoparticles incubated in water alone (lane 3). Error bars = SD.

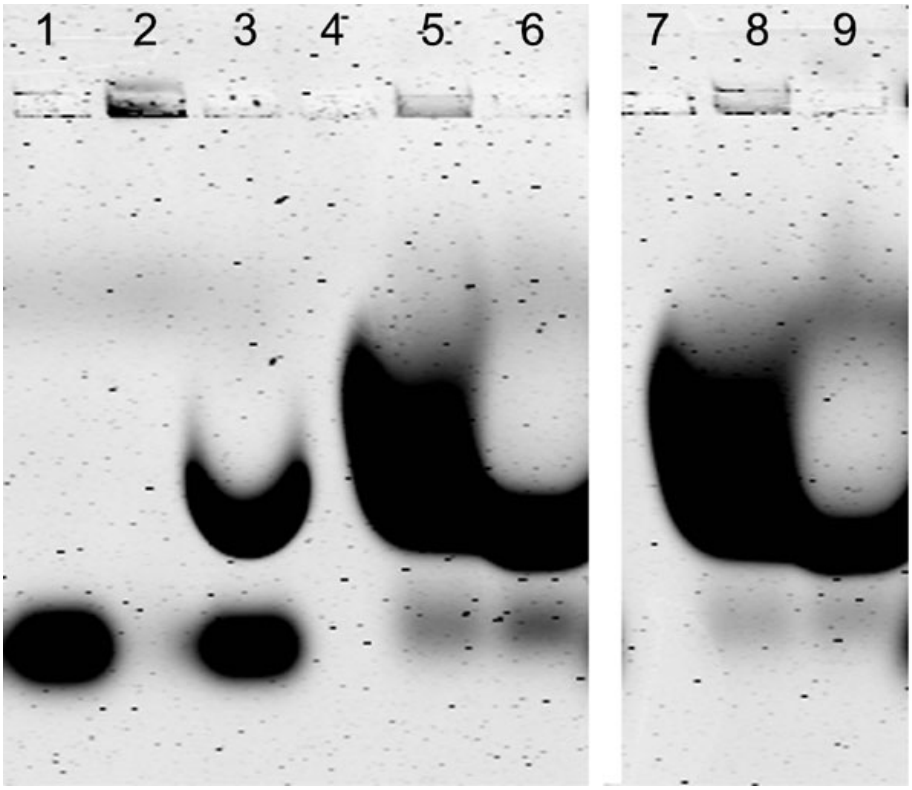

Fig. 13. Gel electrophoresis analysis of urine samples from mice injected with Tf-targeted nanoparticles containing ^{64}Cu-DOTA-siRNA. Lane 1 = Naked unmodified siRNA in water; lane 2, ^{64}Cu-DOTA-siRNA packaged into Tf-targeted nanoparticles (charge ratio (+/-) = 3) in 5% glucose; lane 3, ^{64}Cu-DOTA-siRNA packaged into Tf-targeted nanoparticles (charge ratio (+/-) = 3) in 5% glucose + 1% SDS; lane 4, empty; lane 5, 20 μl urine from a mouse injected with ^{64}Cu-DOTA-siRNA packaged into Tf-targeted nanoparticles (charge ratio (+/-) = 3); lane 6, 20 μl urine from a mouse injected with ^{64}Cu-DOTA-siRNA packaged into Tf-targeted nanoparticles (charge ratio (+/-) = 3) + 1% SDS; lane 7, empty; lane 8, 20 μl urine from an untreated mouse; lane 9, 20 μl urine from an untreated mouse + 1% SDS.

SI Movie 1

Movie 1. Fused microPET/CT images showing tracer uptake over time through all coronal sections after injection of Tf-targeted nanoparticles containing ^{64}Cu-DOTA-siRNA.

SI Movie 2

Movie 2. Rotating fused microPET/CT image of tracer uptake 60 min post injection of Tf-targeted nanoparticles containing ^{64}Cu-DOTA-siRNA.

SI Text

Synthesis and Characterization of DOTA-siRNA.
To verify conjugation of DOTA to the siRNA, a nonradioactive assay was designed to quantify the relative ability of DOTA-siRNA and free DOTA to coordinate gadolinium. Incubation with DOTA-siRNA typically yielded gadolinium binding efficiencies that were ≈50% of that observed for free DOTA.

Because the DOTA-siRNA is also designed to target the luciferase mRNA, its ability to silence luciferase expression in Neuro2A-Luc cells was compared to that of unmodified siRNA against luciferase (SI Fig. 5). Although the unmodified siRNA was able to achieve a maximum luciferase knockdown of >75%, the DOTA-siRNA achieved ≈50% maximum luciferase knockdown, indicating a slight loss in activity after DOTA conjugation. Furthermore, the duration of the knockdown is consistent with an RNAi-based mechanism (1, 2).

Formation of Nanoparticles Containing DOTA-siRNA.
Because conjugation of DOTA to the siRNA molecules may interfere with nanoparticle assembly, dynamic light scattering and gel electrophoresis were used to analyze the nanoparticles formed with DOTA-siRNA. The fraction of the total siRNA that was modified with DOTA had a negligible effect on nanoparticle zeta potential and only a minor effect on nanoparticle size, leading to a slightly larger hydrodynamic diameter as the fraction of DOTA-siRNA was increased (SI Fig. 6). Gel electrophoresis showed that nanoparticles formed with or without DOTA-siRNA had similar migration patterns, and the majority of the siRNA (unmodified or DOTA-conjugated) remained bound within the nanoparticles after formation.

^{64}Cu Labeling of DOTA-siRNA. After labeling the DOTA-siRNA with ^{64}Cu, purification was accomplished using one of two methods: gel filtration or ethanol precipitation. Aliquots of ^{64}Cu-DOTA-siRNA purified by the two methods were separated by gel electrophoresis, and the amount of radioactivity in the bands was quantified by a gamma counter. Relative to the total amount loaded per well, 95% and 90% of the radioactivity was associated with the siRNA band for the ^{64}Cu-DOTA-siRNA purified by gel filtration and ethanol precipitation, respectively. Estimation of the overall yield of the recovery was made using ImageJ analysis of the band intensities, indicating the total amount of siRNA recovered instead of the fraction of the radioactivity in the purification reaction associated with the DOTA-siRNA. Close to 90% of the initial siRNA in the labeling reaction was recovered after ethanol precipitation, whereas only ≈30% of the siRNA was recovered after gel filtration.

Serum Stability of DOTA-siRNA Nanoparticles

Serum Stability of DOTA-siRNA Nanoparticles.
Nanoparticles were formed with unmodified siRNA or with DOTA-siRNA representing either 20% or 50% of the total siRNA in the nanoparticles. All three types of nanoparticles demonstrated essentially equivalent stability against nuclease degradation of the encapsulated siRNA after incubation in mouse serum, with an estimated half-life of ≈11 h (SI Fig. 7). This indicates that the nanoparticle formulations provide stabilization against siRNA nuclease degradation, because naked siRNA duplexes degrade in mouse serum with a half-life of ≈1 h (2).

Gel Electrophoresis of siRNA Nanoparticles Before Injection.
The significant portion of the activity after injection of Tf-targeted nanoparticles that cleared rapidly through the kidneys and was excreted in the urine suggests that free siRNA may have been present. To investigate whether the free siRNA was present before injection, the nanoparticle formulations were analyzed by gel electrophoresis immediately before injection (SI Fig. 10). The nanoparticle formulations showed <10% free siRNA when analyzed on the gel (lane 3 of SI Fig. 10), and this small amount of free siRNA could also be an artifact from the gel electrophoresis procedure. This supports the notion that any residual free siRNA before injection is likely not the dominant factor contributing to the kidney and bladder activity for the nanoparticle formulations.

Gel Electrophoresis of siRNA Nanoparticles After Brief Incubation in Whole Mouse Blood. Gel electrophoresis was used to examine the stability of the nanoparticles against dissociation when incubated briefly in whole mouse blood. Fresh whole mouse blood was extracted from a mouse and added to tubes containing siRNA alone or siRNA nanoparticles. After a brief 5-min incubation, the samples were analyzed by gel electrophoresis (SI Fig. 11). Although the band for naked siRNA incubated in blood (lane 1 of SI Fig. 11) can be seen at the expected position for free siRNA (lane 8 of SI Fig. 11), there is no distinct band corresponding to free siRNA for the nanoparticle formulations incubated in blood (lanes 3 and 5 of SI Fig. 11). Moreover, the band for free siRNA does appear after SDS-mediated disruption of the nanoparticles (lanes 4 and 6 of SI Fig. 11).

Electrolyte Disruption of siRNA Nanoparticles.
Gel electrophoresis was used to examine the stability of the nanoparticles against dissociation when incubated in increasing salt (NaCl) concentrations. As shown in SI Fig. 12*A*, incubation of the siRNA nanoparticles with increasing salt concentrations from 0 to 1.5 M NaCl led to a decrease in the intensity of the band at the top of the gel (siRNA within nanoparticles) with a corresponding increase in the intensity of the free siRNA band at the bottom of the gel (an apparent shift in mobility for free siRNA appears to occur at salt concentrations above ≈1 M). When the same experiment was conducted by using pDNA instead of siRNA as the nucleic acid, the nanoparticles were not as easily disrupted by the presence of NaCl (SI Fig. 12*B*). These results indicate that the siRNA nanoparticles are more susceptible to salt-mediated disruption than pDNA nanoparticles, perhaps owing to the smaller polyanion size for the siRNA relative to plasmid DNA.

Because the nanoparticles are formed by electrostatic interactions between the positively charged cationic polymer strands and the negatively charged siRNA molecules, high salt concentrations can weaken these interactions and allow release of free siRNA. Such high salt concentrations may be experienced by the nanoparticles when traveling through the vasa recta of the kidney. Because of the countercurrent concentrating mechanism used by the kidney, NaCl concentrations in the vasa recta at the papillary tip of the renal medulla can reach ≈0.4 M (3). The results in SI Fig. 12 indicate ≈50% dissociation of the nanoparticles at concentrations of 0.4 M. Additionally, once the free siRNA is released into the complex milieu of the blood, it is not likely to reassociate with the nanoparticles before being bound by other blood components or rapidly cleared by the kidneys (through either glomerular filtration or by active transport by transporters located on the renal proximal tubule cells).

Several previous studies have demonstrated that increasing amounts of NaCl can lead to concentration-dependent dissociation of complexes formed between nucleic acids and cationic polymers or lipids (4-6). Oupicky *et al.*
(5) also showed that polyplexes crosslinked with DTBP (dimethyl-3,3'-dithiobispropionimidate) did not exhibit NaCl-dependent dissociation, and these crosslinked PEGylated polyplexes had prolonged circulation times whereas non-cross-linked PEGylated polyplexes exhibited rapid renal clearance. These observations may indicate that nanoparticle disruption and release of free nucleic acid can contribute to the apparent short circulation times observed for these systemically delivered nanoparticle formulations.

Gel Electrophoresis of Urine Collected After siRNA Nanoparticle Injection.
The urine was collected from mice injected with the siRNA nanoparticles and analyzed by agarose gel electrophoresis to further investigate whether the activity observed in the kidneys and bladder was associated with intact siRNA molecules (SI Fig. 13). Visual inspection of the gel reveals a band near the expected migration distance of free siRNA (lane 5 of SI Fig. 13); however, a faint band is also seen at this same position for urine from mice that were not injected with any siRNA (Lane 8 of SI Fig. 13). Subsequently, each lane was cut into four pieces (top, upper mid, lower mid, bottom), and a gamma counter was used to quantify the radioactivity in each region. At 30 min after injection, ≈20% of the total radioactivity loaded into the lane was associated with the region corresponding to the migration distance of intact siRNA. However, these data cannot confirm whether or not intact ^{64}Cu-DOTA-siRNA contributes to the observed kidney and bladder activity.

1. Bartlett DW, Davis ME (2006) *Nucleic Acids Res* 34: 322-333.

2. Bartlett DW, Davis ME (2007) *Biotechnol Bioeng* 97: 909-921.

3. Edwards A, Delong MJ, Pallone TL (2000) *Am J Physiol Renal Physiol* 278: F257-F269.

4. Eldred SE, Pancost MR, Otte KM, Rozema D, Stahl SS, Gellman SH (2005) *Bioconjugate Chem* 16: 694-699.

5. Oupicky D, Carlisle R, Seymour L (2001) *Gene Ther* 8: 713-724.

6. Pozharski E, MacDonald RC (2003) *Biophys J* 85: 3969-3978.